



Cite this: DOI: 10.1039/c7ob00441a

Croconamides: a new dual hydrogen bond donating motif for anion recognition and organocatalysis†

Anne Jeppesen, Bjarne E. Nielsen, Dennis Larsen,‡ Olivia M. Akselsen, Theis I. Sølling, Theis Brock-Nannestad and Michael Pittelkow*

We introduce bis-aryl croconamides as a new member in the family of dual hydrogen bonding anion receptors. In this study a series of croconamides are synthesised, and the selectivity for anion binding is investigated ($\text{Cl}^- > \text{Br}^- > \text{I}^-$ in CH_2Cl_2). The croconamides exhibit different structures in the crystal phase depending on the substituents on the aromatic rings, and furthermore, the crystal structure revealed the presence of tautomers. DFT calculations elucidated the complex structures formed upon addition of anion to the croconamides, confirming the order of association constants towards the halogen anions. The use of croconamides as organocatalysts in a proof-of-concept study is demonstrated in the formation of THP ethers. In addition to this, construction of a Hammett plot further elucidates the mechanism in action on formation of THP ethers.

Received 16th December 2016,
Accepted 23rd February 2017
DOI: 10.1039/c7ob00441a
rsc.li/obc

Introduction

Dual hydrogen bond donating motifs, such as those found in (thio)ureas and squaramides (Fig. 1), have been studied intensively recently due to their ability to engage in strong hydrogen bonds.^{1–4} The anion recognition capabilities have been utilized in the design of anion transporters (anionophores), anion sensors and in the development of organocatalysts.^{5–7} A structurally simple organocatalyst that has been widely adopted is the thiourea catalyst developed by Schreiner (Fig. 1a),⁸ where the bis-trifluorophenyl groups proved to be particularly important for catalytic activity.⁹ Another well-known dual hydrogen-bonding scaffold is that based on squaramides (Fig. 1b).¹⁰ Squaramides and thioureas have similar dual hydrogen bonding capabilities and the acidic amide hydrogens ($\text{p}K_a = 8.37\text{--}12.48$ vs. $8.5\text{--}13.4$ for comparable squaramide and thiourea structures, respectively, in DMSO) make them powerful anion receptors.^{11–13} Compared to thioureas, these interactions are typically stronger for squaramides, and squaramide-containing structures are also popular organocatalysts.^{14,15}

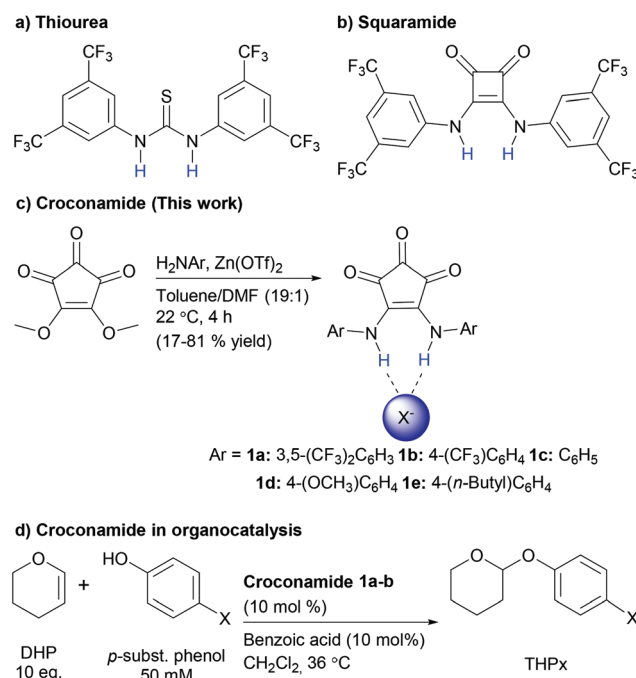


Fig. 1 (a) Example of thiourea, (b) squaramide (c) preparation of *N,N*-bis-aryl croconamides **1a–e**, and (d) the reaction catalysed by croconamides in this work.

Department of Chemistry, University of Copenhagen, Universitetsparken 5, DK-2100 Copenhagen Ø, Denmark. E-mail: pittel@kiku.dk; http://pittelkow.kiku.dk/

† Electronic supplementary information (ESI) available. CCDC 1522925 and 1522926. For ESI and crystallographic data in CIF or other electronic format see DOI: 10.1039/c7ob00441a

‡ Current address: Department of Chemistry, Stanford University, Stanford CA 94305-5017, USA.

These observations led us to consider if the croconic acid analogue to the squaramides, the *croconamides* could possess potent anion recognition and organocatalysis properties

(Fig. 1c). Previous studies on similar croconamide structures are scarce and do not consider the properties investigated here.^{16–21} Here we present the first synthesis of a series of bis-aryl croconamides and explore their abilities to bind anions and, as proof-of-concept, to catalyse the formation of THP ethers (Fig. 1d).

Results and discussion

Synthesis

The bis-aryl croconamides were synthesised from dimethyl croconate and the corresponding anilines (Fig. 1c). Dimethyl croconate is readily available from croconic acid.²² We adapted the zinc triflate mediated reaction protocol developed for squaramides from Taylor and co-workers, and the procedure was successful with a range of electron rich and electron deficient anilines.⁷ For the purpose of anion recognition studies and organocatalysis we focused on the trifluoromethyl substituted derivatives **1a** and **1b**, as these are electron deficient and they are also suitably soluble in organic solvents appropriate for the studies.

Anion recognition

The association properties of **1a** and **1b** towards various anions were investigated in dichloromethane. The continuous variation method (Job's method) indicated a 1:1 binding stoichiometry for all anions tested (see ESI†). The association constants for **1a** towards anions as their tetrabutylammonium (TBA) salts were determined by titration experiments using ¹H NMR or UV/Vis spectroscopy (Table 1). It was convenient to observe the changes in chemical shift for the aromatic CH-protons (protons *a* and *b*, Fig. 2), as these protons experience a significant downfield shift upon addition of anion. During the titration, the signal for the amide protons broadened to such a degree as to make it impractical to monitor these signals (Fig. 2). Due to very strong binding between **1a** and chloride, this association constant could not be accurately determined by a NMR titration and it was therefore determined by a UV/Vis titration.²³ From the absorbance spectra (Fig. 3) several isobestic points are evident indicating that only two species are

Table 1 Association constants for **1a** and **1b** determined by ¹H NMR or UV/Vis titration experiments in CH₂Cl₂. K_a obtained by non-linear regression (see ESI)

	Anion	K_a^d (M ⁻¹)	$\Delta G^\circ e$ (kJ mol ⁻¹)
1	1a Chloride ^a	$1.7 \times 10^6 \pm 3.5 \times 10^5$	-35.4
2	Bromide ^a	$1.9 \times 10^5 \pm 1.3 \times 10^4$	-30.1
3	Iodide ^b	$2.3 \times 10^3 \pm 78$	-19.2
4	Nitrate ^b	$2.3 \times 10^4 \pm 6.7 \times 10^3$	-24.9
5	Hydrogen-sulphate ^b	$2.5 \times 10^3 \pm 2.9 \times 10^2$	-19.4
6	1b Chloride ^a	$1.5 \times 10^6 \pm 5.8 \times 10^4$	-35.3
7	Chloride ^c	10.1 ± 0.07	-5.7

^a Determined by UV/Vis titration. ^b Determined by ¹H NMR titration.

^c In DMSO (0% water). ^d Standard errors on best fit. ^e At 23 °C.

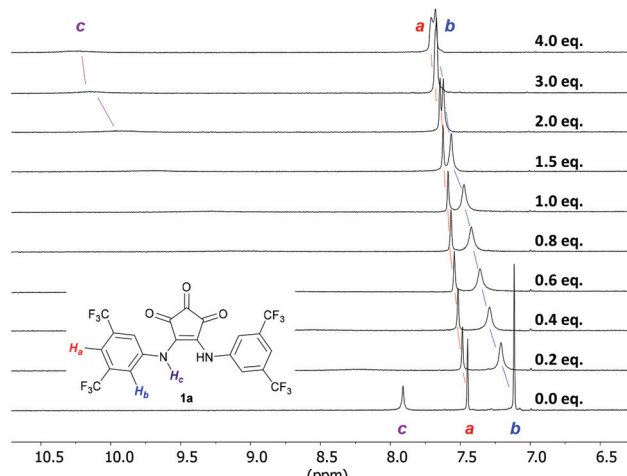


Fig. 2 Changes observed in the ¹H NMR (CD₂Cl₂) of **1a** (1.0 × 10⁻³ M) upon increasing the concentration of TBAI (0–4 × 10⁻³ M).

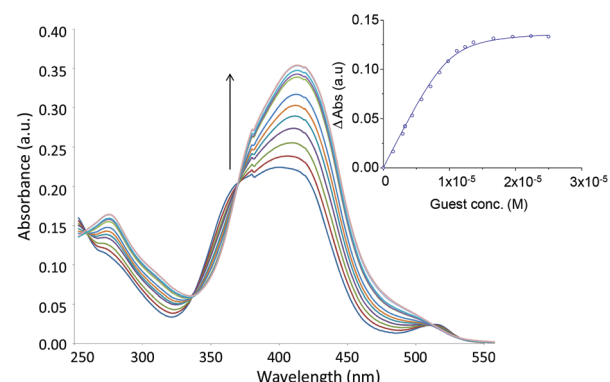


Fig. 3 Absorbance spectra of **1a** (1.0 × 10⁻⁵ M) in CH₂Cl₂ with increasing amounts of TBACl (0–2.5 × 10⁻⁵ M) (change of light source cause an artefact at 380 nm). Inset: Changes in absorbance at 413 nm.

present during the experiment (**1a** and **1a**·Cl⁻), *i.e.* there is no evidence for deprotonation of the croconamide. For the halides the binding strength was in the order: Cl⁻ > Br⁻ > I⁻ towards **1a**. Chloride binding to **1b** was in the same order of magnitude as for **1a**, showing that the number of trifluoromethyl substituents does not have a major effect in this case.

More anions were investigated towards **1a**; nitrate and hydrogensulphate, which both bind strongly to croconamide **1a** with binding affinities of 2.3×10^4 M⁻¹ and 2.5×10^3 M⁻¹, respectively. Titration with TBA acetate led to deprotonisation rather than complexation with anion (see ESI†). To enable a comparison with the binding properties of thiourea- and squaramide-based anion receptors, the binding constant between **1b** and Cl⁻ was determined in anhydrous DMSO (Table 1, entry 7). This binding constant is lower than for the corresponding squaramide obtained in DMSO with 0.5% water ($K_a = 458$ M⁻¹), but of the same order of magnitude as the equivalent thiourea in DMSO ($K_a = 41$ M⁻¹).²⁴ To verify that it is indeed 1:1 complexes formed, upon addition of anions to

croconamides **1a** and **1b**, we fitted the above titration data to a 1 : 2 binding model (see ESI†). The results from the 1 : 2 fits did not give rise to true solutions, or the error on the fit was greater than for the fit to a 1 : 1 binding model. This indicates that the binding stoichiometry is in fact 1 : 1.

X-ray crystal structures

Single crystal X-ray structures of **1a** and **1c** (Fig. 4) were determined to confirm the chemical structures and to gain insight to possible binding modes. In the crystalline state, **1a** shows intramolecular π -stacking of the two aromatic rings. This forces the croconamide to adopt a conformation where the amide hydrogens points in opposite directions, thereby leaving no evidence of the dual hydrogen bond motive in the crystal state. This is not the case for **1c**, where the phenyls are only slightly twisted in opposite directions allowing for intermolecular hydrogen bonding between the center carbonyl group and the amide hydrogens of the neighboring croconamide molecule in the crystal lattice. In addition the crystal structure for **1c** indicated the presence of hydrogen atoms on the carbonyl groups of the cyclopentene trione ring. This could be due to tautomers present in the same crystal structure (Fig. 5). The bond distance of the central carbonyl for **1a** is 1.207 Å and 1.213 Å for croconic acid, whereas it is elongated and measures 1.236 Å for **1c**, suggesting a partial single bond character.²⁵ The mean bond length for a C–O bond in carbonyls in cyclopentanones is 1.208 Å, and for the C–O bond in enols it is 1.333 Å, revealing that the distance measured for **1c** is between the length of a C–O single bond and a C–O double bond.²⁶ The formal C–C double bond in the five-membered ring is 1.401 Å for **1a**, 1.382 Å for croconic acid, and 1.440 Å for **1c**. The mean bond distance for a C–C double bond in cyclopentene is 1.323 Å, implying a partial single

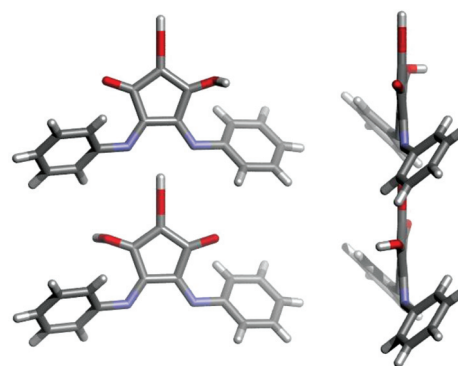


Fig. 5 Crystal structure indicating the presence of tautomers in the crystal phase of **1c**.

bond character for the compounds, which is more expressed for **1c**.

The C–N bonds extending from the ring are 1.341 and 1.347 Å, in **1a**, compared to 1.330 Å for both C–N bonds in **1c**. Although not conclusive, this suggests a partly double bond character for the C–N bonds in **1c**. From this we gather that tautomerisation can occur and is evident in the crystal structure. Despite extensive efforts, we have yet to obtain crystal structures of anion conjugates of either of the croconamides. It is important to stress that in solution we observe symmetrical NMR spectra indicating the dual hydrogen bond motif is indeed present for all croconamide structures.

DFT-calculations

Previously, the dipole moment and hyperpolarisabilities have been calculated for various croconamides.²¹ We wished to perform DFT calculations, as these can give important insight into the structure of supramolecular complexes. We calculated the energy of complexation for **1c**, the corresponding squaramide and thiourea with the halides chloride, bromide, and iodide. Both the simple B3LYP/MidiX and the advanced G4MP2 level was explored (Table 2 and ESI†). The favorable energy of complexation is in the order $\text{Cl}^- > \text{Br}^- > \text{I}^-$ and squaramide > croconamide > thiourea. The calculations, thus, are in accordance with the experimental data. The G4MP2-

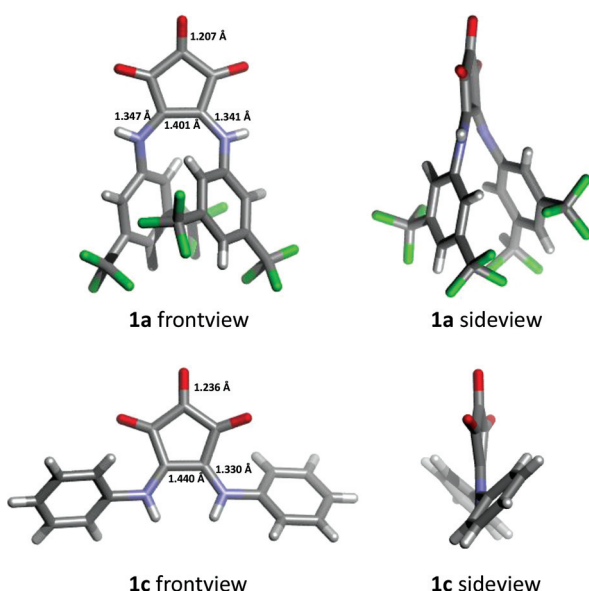


Fig. 4 Single crystal X-ray structures of **1a** (top) and **1c** (bottom).

Table 2 DFT calculated energies of complexation in the gas phase, B3LYP/MidiX and G4MP2

Catalyst	Energy of complexation, ΔE^a (kJ mol ⁻¹)		
	Cl^-	Br^-	I^-
B3LYP/MidiX			
1 Croconamide	-285.4	-238.6	-163.1
2 Squaramide	-293.0	-248.6	-174.6
3 Thiourea	-267.8	-226.6	-161.0
G4MP2			
4 Croconamide	-209.5	-185.2	—

^a See ESI for details of the calculations.

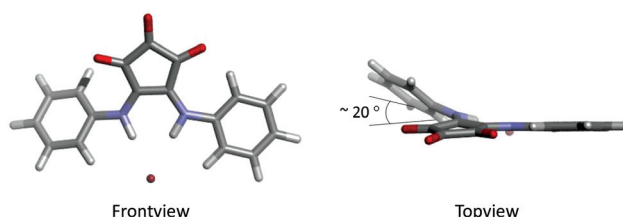


Fig. 6 Front and side views of the calculated complexation of **1c** with bromide.

level calculations (Table 2, entry 4), shows the same trend as the lower level of calculations (B3LYP/MidiX). Structural information can also be obtained from the calculations, and a twisting of the anilines with regards to the central five-membered ring is observed (Fig. 6). For complexation with chloride and bromide one aniline was almost in plane with the central aromatic ring (torsional angle $\sim 6\text{--}9^\circ$) while the second aniline was twisted out of the plane (torsional angle $\sim 20^\circ$). For iodide, the two anilines were twisted out of the plane in opposite directions with a torsional angle $\sim 19^\circ$ for both anilines. Complexation with iodide forces the conjugated system of the croconamide out of planarity, which is highly unfavorable. This is in agreement with the order of binding for the halides, with the smaller chloride resulting in the strongest association.

Organocatalysis

We sought to elucidate the ability of croconamides to act as organocatalysts, and we chose the tetrahydropyranylation of phenols as our model reaction (Table 3). Schreiner's catalyst has previously been used to catalyse this reaction.^{27,28} The results are listed in Table 3, entries 1–3. The studied catalysts **1a** catalyses the reaction with the highest rate, $3.74 \times 10^{-5} \text{ M}^{-1} \text{ s}^{-1}$, **1b** is slightly less efficient ($1.06 \times 10^{-5} \text{ M}^{-1} \text{ s}^{-1}$). This implies that the number of trifluoromethyl groups does have an

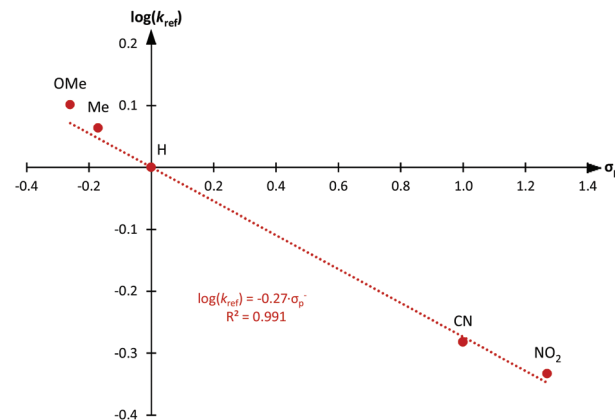


Fig. 7 Hammett plot for *p*-substituted phenols in tetrahydropyranylation with catalyst **1a**.

impact on the croconamides' ability to catalyse the reaction. Schreiner's catalyst works very well for this reaction when the reaction is performed in neat DHP, but not under the dilute conditions applied here, where we did not observe any conversion.²⁷ Structure **1a** do, however, catalyse the reaction with a higher rate than with Schreiner's catalyst or with benzoic acid alone (no catalyst present), which did not result in product formation. To gain further insight to the reaction catalysed by **1a**, a series of *p*-substituted phenols were tested in the tetrahydropyranylation reaction (Table 3, entries 4–8). The obtained rate constants and σ_p^- values were used to obtain a Hammett plot with good linear correlation (Fig. 7). The negative slope ($\rho = -0.27$) indicates that electron donating substituents on the aromatic ring of the phenol facilitate the reaction, and a decrease in electron density on the phenol occurs in the transition state. This could either be in the form of build-up of positive charge or loss of negative charge. This fits with the oxygen on the phenol taking part in a non-covalent bond in the transition state, indicating that the mechanism involves an organised complexation of the phenol with DHP and the catalyst.

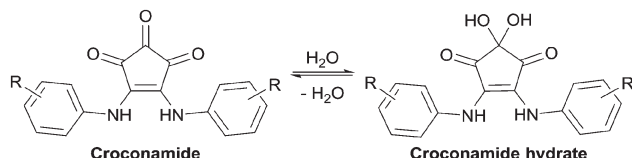
Acidity

The $\text{p}K_a$ values were determined for **1a** and **1b** in DMSO to 11.5 and 10.8 respectively (see ESI†). We expected catalyst **1a** to possess more acidic croconamide protons than **1b**, as **1a** has two CF_3 -groups per aryl group, and **1b** only one. This would be in agreement with **1a** being the most effective catalyst, if the croconamides enable the reaction *via* the dual hydrogen bonding motif, as is the case for similar thiourea catalysts.²⁴ The explanation for this unexpected result is that the more electron deficient the aryl-substituent are, the more prone the croconamide is to be present as the corresponding hydrate on the central carbonyl group (Scheme 1). This phenomenon is conveniently observable in DMSO solution (the solvent used to measure the $\text{p}K_a$ value) where water is often present, but less so in CH_2Cl_2 solution (the solvent used for the catalysis experiments). When leaving a sample of **1a** in 0.5 vol% water in

Table 3 Tetrahydropyranylation reaction. k_2 obtained by non-linear regression (see ESI)

	DHP 10 eq.	<i>p</i> -subst. phenol 50 mM	Catalyst (10 mol%) Benzoic acid (10 mol%) CH_2Cl_2 , 36 °C	THPx
Catalyst		<i>p</i> -Subst. phenol		$k_2^a (\times 10^{-5} \text{ M}^{-1} \text{ s}^{-1})$
1 1a		-OMe		3.74 ± 0.03
2 1b		-OMe		1.06 ± 0.04
3 Schreiner's catalyst		-OMe		No conversion
4 1a		-OMe		3.44 ± 0.05
5 1a		-Me		3.15 ± 0.13
6 1a		-H		2.72 ± 0.06
7 1a		-CN		1.42 ± 0.02
8 1a		-NO ₂		1.264 ± 0.019

^a Obtained by non-linear regression (see ESI).



Scheme 1 Formation of croconamide hydrate.

DMSO, the formation of the hydrate can be observed using ^1H NMR spectroscopy. After 48 hours the samples has reached equilibrium, where half of **1a** is present as the hydrate. In the case of **1b**, only 35% existed as the hydrate after 48 hours. The identities of the hydrates were confirmed with LC-MS analysis. For the corresponding squaramide to **1a** the $\text{p}K_{\text{a}}$ value is 8.37 in DMSO,¹³ which means that the croconamide **1a** is less acidic than its squaramide analogue.

Conclusions

To conclude, we have introduced a new dual hydrogen bond motif, the croconamides, and we have illustrated how this new motif can be used for both anion recognition and organocatalysis. We are currently exploring further functionalisation of these structures and the preparation of unsymmetrical croconamide structures with the aim of enabling strong anion binding and further applications in catalysis.

Experimental

General

All chemicals were purchased from commercial suppliers and used as received unless otherwise stated. Dimethyl croconate was synthesised according to the procedure by Williams,²² and barium croconate for this synthesis was synthesised by SunChemicals. For synthesis and kinetic studies HPLC grade solvents were used, for kinetic studies these were dried using molecular sieves (4 Å). For UV/Vis titrations spectroscopic grade solvents were used, and dimethyl sulfoxide was dried by standing over molecular sieves (4 Å) prior to use.

A Bruker Ultrashield Plus 500 spectrometer with a Cryoprobe was used to record NMR spectra of the synthesised compounds. The spectrometer operated at 500 MHz for ^1H and 126 MHz for ^{13}C . For ^{19}F and titrations a Bruker Avance 3 spectrometer with a BBFO probe was used, operating at 470 MHz for ^{19}F , 500 MHz for ^1H and 126 MHz for ^{13}C . The spectrometers operated at 20 °C and all spectra were referenced to the internal solvent residue for ^1H and ^{13}C , and to trifluoroacetic acid in a sealed tube for ^{19}F . The ^{19}F spectrum for the Schreiner catalyst, however, was recorded on an Oxford NMR 300 spectrometer, operating at 282 MHz. MestReNova version 10.0.2 from MestreLab Research S.L. was used to process the NMR data. Standard 1D and 2D NMR techniques

(COSY, ^{13}C APT, HSQC (for ^1H and ^{13}C), and HMBC (for ^1H and ^{13}C) was used to assign ^1H and ^{13}C resonances.

UV/Vis measurements were performed using a PerkinElmer UV/Vis spectrometer Lamda 2. HPLC analysis was carried out on a Dionex UltiMate 3000, which was coupled to an UltiMate 3000 diode array UV/Vis detector that measured absorbance of light between 190–800 nm.

LC-MS analysis were obtained by coupling the above mentioned HPLC apparatus with a Bruker MicrOTOF-QII system equipped with an ESI source.

Synthesis

4,5-Bis((3,5-bis(trifluoromethyl)phenyl)amino)cyclopent-4-ene-1,2,3-trione (1a). Dimethylcroconate (500 mg, 2.94 mmol) and $\text{Zn}(\text{OTf})_2$ (214 mg, 0.587 mmol) was suspended in toluene/DMF (19 : 1, 10 ml) and 3,5-bis(trifluoromethyl)aniline (1.35 g, 0.9 ml, 5.9 mmol) was added. The flask was fitted with a stopper and the reaction was stirred at room temperature for four hours. The reaction mixture was evaporated to dryness, redissolved in ethylacetate and evaporated on Celite (25 g) for purification using dry column vacuum chromatography. A column of 4 cm in diameter charged with 4 cm silica gel, a gradient of 2.5% ethyl acetate in heptane was used. The gradient was held constant from 10% ethyl acetate in heptane, and all fractions were 50 ml. Fraction 13 to 37 was evaporated, and the isolated material was recrystallised from dichloromethane to yield **1a** as an orange solid (503 mg, 30%), decompose above 250 °C. ^1H NMR (500 MHz, $\text{DMSO}-d_6$) δ 10.72 (s, 2H), 7.39 (s, 2H), 7.19–7.16 (m, 4H). ^{13}C NMR (126 MHz, $\text{DMSO}-d_6$) δ 186.54, 181.27, 142.42, 139.12, 129.86 (q, $J = 33.2$ Hz), 122.77 (q, $J = 273.0$ Hz), 121.19, 116.12. ^{19}F NMR (470 MHz, $\text{DMSO}-d_6$) δ –60.52. LC-HRMS: $m/z = 563.0276 [\text{M} - \text{H}^+]$ (Calculated 563.0271).

4,5-Bis((4-(trifluoromethyl)phenyl)amino)cyclopent-4-ene-1,2,3-trione (1b). Dimethylcroconate (200 mg, 1.18 mmol) and $\text{Zn}(\text{OTf})_2$ (85 mg, 0.236 mmol) was suspended in toluene/DMF (19 : 1, 10 ml) and 4-(trifluoromethyl)aniline (400 mg, 2.5 mmol) was added. The flask was fitted with a stopper and the reaction was stirred at room temperature for four hours. The reaction mixture was evaporated to dryness, redissolved in ethylacetate and evaporated on Celite (20 g) for purification using dry column vacuum chromatography. A column of 4 cm in diameter charged with 4 cm silica gel, a gradient of 5% ethyl acetate in heptane was used. Fraction 10 to 13 were evaporated, and the isolated material was recrystallised from chloroform to yield **1b** as an orange solid (85 mg, 17%), decompose above 260 °C. ^1H NMR (500 MHz, $\text{DMSO}-d_6$) δ 10.43 (s, 2H), 7.27 (d, $J = 8.5$ Hz, 4H), 6.84 (d, $J = 8.5$ Hz, 4H). ^{13}C NMR (126 MHz, $\text{DMSO}-d_6$) δ 186.09, 180.93, 143.76, 141.14, 124.13 (q, $J = 271.2$), 124.88, 123.73 (q, $J = 32.2$), 121.77. ^{19}F NMR (470 MHz, $\text{DMSO}-d_6$) δ –59.04. LC-HRMS: $m/z = 427.0525 [\text{M} - \text{H}^+]$ (Calculated 425.0523).

4,5-Bis(phenylamino)cyclopent-4-ene-1,2,3-trione (1c). Dimethylcroconate (200 mg, 1.18 mmol) and $\text{Zn}(\text{OTf})_2$ (85 mg, 0.236 mmol) was suspended in toluene/DMF (19 : 1, 10 ml) and aniline (230 mg, 225 μl , 2.47 mmol) was added. The flask

was fitted with a stopper and the reaction was stirred at room temperature for four hours. Hereafter, dichloromethane (20 ml) was added and the precipitate was centrifuged down and washed several times with ethyl acetate (7×40 ml) to yield **1c** as a dark red solid (194 mg, 56%), decompose above 240 °C. ^1H NMR (500 MHz, DMSO- d_6) δ 10.07 (s, 2H), 7.03–7.00 (m, 4H), 6.90–6.87 (m, 2H), 6.75 (d, $J = 7.6$ Hz, 4H). ^{13}C NMR (126 MHz, DMSO- d_6) δ 186.04, 180.20, 145.26, 137.51, 127.84, 124.07, 122.06. LC-HRMS: $m/z = 291.0778$ [M – H $^+$] (Calculated 291.0775).

4,5-Bis((4-methoxyphenyl)amino)cyclopent-4-ene-1,2,3-trione (1d). Dimethylcroconate (200 mg, 1.18 mmol) and Zn(OTf) $_2$ (85 mg, 0.236 mmol) was suspended in toluene/DMF (19 : 1, 10 ml) and *p*-anisidine (304 mg, 2.47 mmol) was added. The flask was fitted with a stopper and the reaction was stirred at room temperature for four hours. The mixture was evaporated to dryness, and the resulting crude was dissolved in methanol (30 ml) to which was added diethyl ether (50 ml). The precipitate was centrifuged down and washed several times with diethyl ether (4×15 ml) to yield compound **1d** (337 mg, 81%) as a dark red solid, decompose above 250 °C. ^1H NMR (500 MHz, DMSO- d_6) δ 9.94 (s, 2H), 6.69 (d, $J = 8.9$ Hz, 4H), 6.60 (d, $J = 8.9$ Hz, 4H), 3.67 (s, 6H). ^{13}C NMR (126 MHz, DMSO- d_6) δ 185.47, 179.99, 156.51, 145.72, 130.65, 123.80, 113.28, 55.32. LC-HRMS: $m/z = 351.0989$ [M – H $^+$] (Calculated 351.0986).

4,5-Bis((4-butylphenyl)amino)cyclopent-4-ene-1,2,3-trione (1e). Dimethylcroconate (200 mg, 1.18 mmol) and Zn(OTf) $_2$ (85 mg, 0.236 mmol) was suspended in toluene/DMF (19 : 1, 10 ml) and 4-butylaniline (0.37 ml, 2.5 mmol) was added. The flask was fitted with a stopper and the reaction was stirred at room temperature for four hours. The mixture was evaporated to dryness, and the resulting crude dissolved in methanol (40 ml) to which was added diethyl ether (50 ml). The precipitate was centrifuged down and washed several times with diethyl ether (4×15 ml) to yield **1e** (220 mg, 46%) as a dark solid, mp. 233–234 °C. ^1H NMR (500 MHz, DMSO- d_6) δ 10.06 (s, 2H), 6.77 (d, $J = 8.3$ Hz, 4H), 6.60 (d, $J = 8.3$ Hz, 4H), 2.39 (t, $J = 7.6$ Hz, 4H), 1.49–1.40 (m, 4H), 1.23–1.30 (m, 4H), 0.91 (t, $J = 7.3$ Hz, 6H). ^{13}C NMR (126 MHz, DMSO- d_6) δ 185.56, 180.42, 145.27, 138.27, 135.19, 127.60, 122.04, 34.26, 33.15, 21.63, 13.82. LC-HRMS: $m/z = 405.2171$ [M – H $^+$] (Calculated 405.2173).

Bis(3,5-bis[trifluoromethyl]phenyl) thiourea (Schreiner's catalyst).²⁸ 3,5-Bis(trifluoromethyl)aniline (165 mg, 0.718 mmol, 1.2 eq.) was dissolved in CHCl $_3$ (5.0 mL) and 3,5-bis(trifluoromethyl)phenyl isothiocyanate (163 mg, 0.601 mmol, 1.0 eq.) was added. Acetonitrile (2.0 mL) was added and the resulting clear solution was heated under reflux for 40 hours after which all of the solvent was removed under reduced pressure. The white residue was recrystallized from boiling chloroform (9 mL) to yield the title compound as white needles (292 mg, 97%), mp. 174–175 °C. ^1H NMR (500 MHz, DMSO- d_6) δ = 10.64 (s, 2H), 8.20 (s, 4H), 7.87 (s, 2H). ^{13}C NMR (126 MHz, DMSO- d_6) δ = 180.59, 141.15, 130.34 (q, $J = 32.7$), 124.16, 123.16 (q, $J = 272.3$), 117.79. ^{19}F NMR (282 MHz,

DMSO- d_6) δ = -59.77. Elemental analysis for C₁₇H₈F₁₂N₂S: Found (calculated) 41.15% C (40.81), 1.48% H (1.61), 5.60% N (5.60). LC-HRMS: 501.0292 [M + H $^+$] (Calculated 501.0289).

Acknowledgements

We acknowledge financial support from the Lundbeck Foundation for a Young Group Leader Fellowship (MP), the Carlsberg Foundation for a postdoc grant (DL), the Innovation Fund Denmark and Department of Chemistry, University of Copenhagen for a PhD scholarship (AJ).

Notes and references

- Z. Zhang and P. R. Schreiner, *Chem. Soc. Rev.*, 2009, **38**, 1187–1198.
- V. Amendola, L. Fabbrizzi and L. Mosca, *Chem. Soc. Rev.*, 2010, **39**, 3889–3915.
- J. Alemán, A. Parra, H. Jiang and K. A. Jørgensen, *Chem. – Eur. J.*, 2011, **17**, 6890–6899.
- M. Tsakos and C. G. Kokotos, *Tetrahedron*, 2013, **69**, 10199–10222.
- N. Busschaert, R. B. P. Elmes, D. D. Czech, X. Wu, I. L. Kirby, E. M. Peck, K. D. Hendzel, S. K. Shaw, B. Chan, B. D. Smith, K. A. Jolliffe and P. A. Gale, *Chem. Sci.*, 2014, **5**, 3617–3626.
- R. B. P. Elmes, P. Turner and K. A. Jolliffe, *Org. Lett.*, 2013, **15**, 5638–5641.
- A. Rostami, A. Colin, X. Y. Li, M. G. Chudzinski, A. J. Lough and M. S. Taylor, *J. Org. Chem.*, 2010, **75**, 3983–3992.
- P. R. Schreiner and A. Wittkopp, *Org. Lett.*, 2002, **4**, 217–220.
- A. Wittkopp and P. R. Schreiner, *Chem. – Eur. J.*, 2003, **9**, 407–414.
- Y. Geng, H. M. Faidallah, H. A. Albar, I. A. Mhkalid and R. R. Schmidt, *Eur. J. Org. Chem.*, 2013, 7035–7040.
- M. H. Al-Sayah and N. R. Branda, *Thermochim. Acta*, 2010, **503–504**, 28–32.
- G. Jakab, C. Tancon, Z. Zhang, K. M. Lippert and P. R. Schreiner, *Org. Lett.*, 2012, **14**, 1724–1727.
- X. Ni, X. Li, Z. Wang and J.-P. Cheng, *Org. Lett.*, 2014, **16**, 1786–1789.
- S. J. Edwards, H. Valkenier, N. Busschaert, P. A. Gale and A. P. Davis, *Angew. Chem. Int. Ed.*, 2015, **54**, 4592–4596.
- J. Liu, C. Chen, Z. Li, W. Wu, X. Zhi, Q. Zhang, H. Wu, X. Wang, S. Cui and K. Guo, *Polym. Chem.*, 2015, **6**, 3754–3757.
- B. Eistert, H. Fink and H.-K. Werner, *Liebigs Ann. Chem.*, 1962, **657**, 131–141.
- S. Skujins and G. A. Webb, *Tetrahedron*, 1969, **25**, 3947–3954.
- S. Skujins, J. Delderfield and G. A. Webb, *Tetrahedron*, 1969, **25**, 3935–3945.
- J. Fabian and H. Junek, *Monatsh. Chem.*, 1985, **116**, 625–632.

- 20 G. Seitz, J. Auch and W. Klein, *Chem.-Ztg.*, 1987, **111**, 343–344.
- 21 J. O. Morley, *J. Mol. Struct. Theochem.*, 1995, **357**, 49–57.
- 22 R. F. X. Williams, *Phosphorus, Sulfur Silicon Relat. Elem.*, 1976, **2**, 141–146.
- 23 P. Thordarson, *Chem. Soc. Rev.*, 2011, **40**, 1305–1323.
- 24 N. Busschaert, I. L. Kirby, S. Young, S. J. Coles, P. N. Horton, M. E. Light and P. A. Gale, *Angew. Chem., Int. Ed.*, 2012, **51**, 4426–4430.
- 25 D. Braga, L. Maini and F. Grepioni, *Chem. – Eur. J.*, 2002, **8**, 1804–1812.
- 26 F. H. Allen, O. Kennard, D. G. Watson, L. Brammer, A. G. Orpen and R. Taylor, *J. Chem. Soc., Perkin Trans. 2*, 1987, 1–19.
- 27 M. Kotke and P. R. Schreiner, *Synthesis*, 2007, 779–790.
- 28 Y.-B. Huang and C. Cai, *J. Chem. Res.*, 2009, **2009**, 686–688.